

Distinct order of Gd 4f and Fe 3d moments coexisting in GdFe_4Al_8

M. Angst,* A. Kreyssig,[†] Y. Janssen, J.-W. Kim, L. Tan, D. Wermeille,

Y. Mozharivskyij, A. Kracher, A. I. Goldman, and P. C. Canfield

Ames Laboratory DOE and Department of Physics and Astronomy, Iowa State University, Ames, IA 50011, USA

(Dated: February 8, 2020)

Single crystals of flux-grown GdFe_4Al_8 were characterized by thermodynamic, transport, and x-ray resonant magnetic scattering measurements. In addition to antiferromagnetic order at $T_N \approx 155$ K, two low temperature transitions at $T_1 \approx 21$ K, $T_2 \approx 27$ K were identified. Fe moments order at T_N with incommensurate propagation vector $(\tau, \tau, 0)$ with $\tau = 0.06 - 0.14$, and maintain this order over the entire $T < T_N$ range. Gd 4f moments order only below T_2 , and apparently do not follow the Fe-moment modulation. Below T_1 an antiferromagnetic component with $(0, 0, 0.3)$ modulation is present.

PACS numbers: 75.25.+z, 75.30.-m

Understanding the interplay of rare-earth local-moment magnetism and 3d transition metal itinerant magnetism is of fundamental physical interest¹ and may help in the design of efficient permanent magnets. The tetragonal RFe_4Al_8 (R=rare earth) compounds (Fig. 1 inset) are well suited for studying this interplay because of simple symmetry conditions and because the interaction between the two magnetic subsystems is rather weak: Fe moments seem to order without a corresponding R 4f order. Consequently, numerous studies have been performed on RFe_4Al_8 (R148) over the last 30 years and interest in these compounds has remained high.^{2,3,4,5,6,7,8,9,10,11}

Neutron-scattering studies performed on R148 with various R indicate that Fe moments, between which the coupling is strongest, order between 100 and 200 K, generally in cycloidal structures with propagation $\parallel [110]$ and moments confined to the (001) plane.^{8,9,10,11} For magnetic R, ordering of the R moments, with much weaker coupling and at much lower temperature T , was reported. However, this ordering was found to progress as rather drawn-out crossovers. For example in Dy148 there is a magnetization rising faster than $(T - T')^{-1}$, but there are no sharp features.⁸ No additional low- T magnetic-propagation vectors were found. Furthermore, the R moments were found to follow the Fe-moment modulation.^{8,10} This implies that the Fe-R moment interaction is rather strong compared to the R-R moment interaction, while both these interactions are much weaker than the Fe-Fe moment interaction.

Of all R, Gd has two advantages associated with its high-spin (S) and zero-angular-momentum (L) 4f state: 1) high S results in strong magnetic coupling between the localized 4f and the conduction electrons, implying large magnetic interactions giving Gd the largest de Gennes factor of all R; 2) $L = 0$ implies a spherical 4f charge-cloud and no magneto-crystalline anisotropy (MCA) resulting from crystal-electric-field effects – the direct interplay of magnetic interactions can be studied without MCA. In view of this, it is somewhat surprising that GdFe_4Al_8 (Gd148) has been much less studied^{4,5} than R148 with other rare earths. In particular, apart from

Mössbauer spectroscopy,² there have been no microscopic studies on Gd148.

Here, we report on measurements on single-crystalline GdFe_4Al_8 including magnetization, electrical transport, specific heat, x-ray diffraction, as well as preliminary synchrotron x-ray resonant magnetic scattering (XRMS) data. We provide evidence for two consecutive phase transitions at low T in addition to the Néel transition at 155 K, and show that the two low- T transitions are associated with the ordering of the Gd 4f moments in complex magnetic structures likely involving both ferro- and antiferromagnetic components. In contrast to other R148 compounds, the 4f-moment ordering is associated with a propagation vector that is distinct from the vector associated with the Fe moment order, which keeps its character over the whole $T < T_N$ range.

We have grown single crystals of Gd148 with a self-flux method,^{12,13,14} using an alloy with composition $\text{Gd}_3\text{Fe}_{16}\text{Al}_{34}$, which was heated to 1475°C and then slowly (2°C/h) cooled to 1180°C, at which point the flux was decanted.¹⁵ Crystals typically grow prismatically (long direction up to 1 cm $\parallel [001]$) with [110] facets. We determined, via x-ray-diffraction-structure refinement and electron-microprobe analysis, the crystals to be slightly iron deficient, but detected no Al on Fe sites or vice versa.

Since the exact iron stoichiometry may vary slightly from crystal to crystal,¹⁵ all measurements presented here were performed on the same crystal, which has a refined composition $\text{GdFe}_{3.96(1)}\text{Al}_8$ ($a = 8.770 \text{ \AA}$, $c = 5.044 \text{ \AA}$). A bar cut from the crystal by a wire saw was connected with contacts for 4-point electrical-transport measurements with the current $j \parallel [110]$ (sample A). On a second bar cut from the crystal (sample B) we measured magnetization and specific heat. The above measurements were performed with a commercial (Quantum Design) laboratory equipment. Sample B was also used in the XRMS experiment, performed on the MUCAT undulator beamline at the Advanced Photon Source, Argonne National Laboratory.

In Fig. 1, we show the T dependence of the resistivity ρ ($j \parallel [110]$) and of the inverse dc-susceptibility χ^{-1} , as

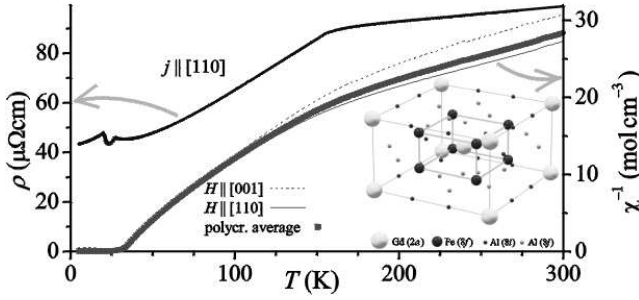


FIG. 1: (Color online) Zero-field resistivity ρ (along [110]) and inverse dc susceptibility χ^{-1} vs temperature T . Inset: Crystal structure of GdFe_4Al_8 .

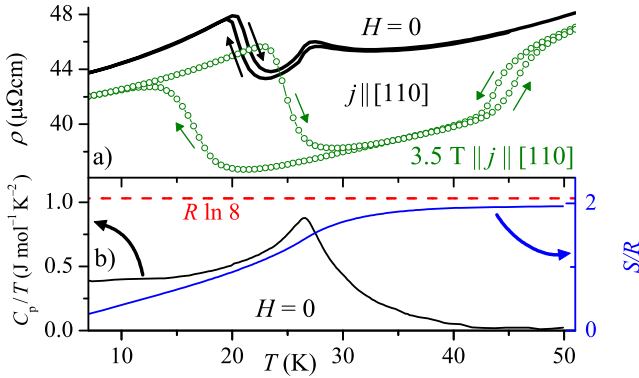


FIG. 2: (Color online) Diverse quantities as a function of temperature T in the range $7 - 51\text{ K}$. Arrows indicate the direction of T change. a) resistivity ρ along [110] in $H = 0$ (thick black line) and in $3.5\text{ T} \parallel j \parallel [110]$ (circles). b) 4f moment contribution to specific heat C_p and corresponding entropy S . Dashed line: full Gd 4f entropy.

determined from magnetization $M(T)$ in a field of 0.1 T , below which M vs field H is linear for $T \gtrsim 40\text{ K}$. The antiferromagnetic ordering at $T_N = 155\text{ K}$ is visible as a sharp kink in $\rho(T)$.¹⁶ In agreement with measurements on polycrystalline samples,² χ follows Curie-Weiss laws both above and, over a limited T range, below T_N . We found (on the calculated polycrystalline average) similar parameters, but for $T < T_N$, our corresponding effective moment ($7.4\text{ }μ_B/\text{f.u.}$) is closer to the Gd free-ion value ($7.9\text{ }μ_B/\text{f.u.}$) than the one reported by Buschow *et al.*² ($6.2\text{ }μ_B/\text{f.u.}$).

The resistivity curve shows additional features just below 30 K , magnified in Fig. 2a) (lines): The broad peak in $\rho(T)$ at $\sim 28\text{ K}$ with a drop at $\sim 26.5\text{ K}$ (T_2) indicates a phase transition. Furthermore, with decreasing T , at $\sim 21\text{ K}$ (T_1) there is a sudden increase by 10% of ρ . This feature is hysteretic in temperature, suggesting a first order transition.¹⁷

Figure 2b) shows the specific heat C_p/T after subtraction of the mass-scaled specific heat¹⁸ of YFe_4Al_8 . Since the necessary mass-scaling is small, the remaining specific heat is close to the magnetic contribution associated with the Gd sublattice. The broad, asymmetric, peak at

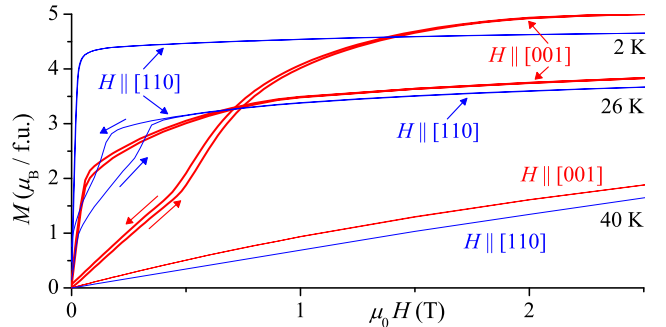


FIG. 3: (Color online) Magnetization M as a function of field H at selected T , $H \parallel [110]$ (blue) and $H \parallel [001]$ (red).

$\sim 26.5\text{ K}$ corresponds to the drop in ρ at T_2 . No feature in the specific heat is visible around T_1 . We checked the specific-heat raw data, and can exclude any latent heat restricted to a temperature region smaller than the spacing of measurement points. We conclude that the latent heat of the T_1 transition has to be small, i.e., the phases above and below T_1 have similar entropies.

The corresponding magnetic entropy S , obtained by integration, is also shown. At 30 K S already reaches over 80% of the full entropy of Gd 4f moments ($R \ln 8$, dashed line) and above 45 K it hardly varies anymore, having reached $> 93\%$ of the full 4f entropy. This strongly suggests that the Gd 4f moments are not ordered above T_2 , and the transition at T_2 corresponds to the ordering of the 4f moments.

Application of $H \parallel j \parallel [110]$ enhances the magnitude of the jump of ρ at T_1 and greatly increases the hysteresis in temperature, making the first order nature of the transition more apparent [Fig. 2a) o]. The average ($T \uparrow, T \downarrow$) temperature of the T_1 feature, however, is only weakly suppressed. In contrast to this, the T_2 feature is shifted to higher T by $H \parallel [110]$, suggesting a ferromagnetic nature of the phase at $T < T_2$. Furthermore, $H \parallel [110]$ removes the peak in ρ just above the drop, and causes the feature to exhibit hysteresis. This different response to $H \parallel [110]$ demonstrates that there are two independent magnetic transitions T_1 , T_2 , dividing the ordered state below T_N into three phases, a low-temperature (LTP), an intermediate-temperature (ITP), and a high-temperature (HTP) phase.

In order to investigate the magnetic nature of these phases, we measured the magnetization M as a function of T and H ($\parallel [110]$ and $\parallel [001]$). In Fig. 3, we display $M(H)$ loops at selected T . For $H \parallel [110]$, at 40 K , $M(H)$ shows almost linear behavior, but at 2 K $M(H)$ has a behavior typical for soft ferromagnets: saturation in a field which is of the order of the estimated demagnetizing field, but no hysteresis or remanence. However, the saturation value of $4.5\text{ }μ_B/\text{f.u.}$ at 2 K is much lower than the full Gd moment of $7\text{ }μ_B/\text{f.u.}$. At 26 K , pronounced hysteresis is visible in low H . This is ubiquitous for $M(H)$ in the ITP. Whether this corresponds to a metamagnetic transition present only in the ITP or is due to, e.g., domain effects

remains to be clarified. In any case, the magnetization both in the LTP and in the ITP is consistent with the presence of a spontaneous ferromagnetic in-plane component. The LTP-to-ITP transition in $M(H)$, $H \parallel [110]$ is accompanied by a drop of the spontaneous moment to $\sim 1 \mu_B$, and by the appearance of hysteresis.

For $H \parallel [001]$ at 26 K (ITP), the form of $M(H)$ is consistent with a spontaneous ferromagnetic moment of about $2 \mu_B$. For the LTP consider $M(H)$ at 2 K. Below 0.5 T, $M(H)$ is linear, above it rises more strongly before slowly starting to saturate. The saturation value of $M < 5 \mu_B/\text{f.u.}$ is higher than for $H \parallel [110]$, but still far below the full Gd 4f moment. Note that the difference to $7 \mu_B/\text{f.u.}$ is much too large to be explained by a negative contribution of the Gd conduction electrons. The low saturated moment implies that the magnetization does *not correspond to the magnetization of a simple ferromagnet*.

The linear $M(H)$ behavior (below 0.5 T) may be due to an antiferromagnetic modulation with staggered moment in [001] direction. Alternatively, the ITP-to-LTP transition could correspond to a reorientation of ferromagnetically aligned 4f moments (as suggested in Ref. 4) without involvement of an additional antiferromagnetic modulation. The drastic increase in $\rho(T)$ when crossing from the ITP to the LTP is, however, more common for an antiferromagnetic transition.^{19,20,21}

In the preliminary x-ray resonant magnetic scattering (XRMS)^{22,23,24} experiment using polarization analysis, we found magnetic satellite reflections with modulation vector $(\tau, \tau, 0)$, $0.06 \leq \tau \leq 0.135$ depending on T , around the $(4, 4, 0)$ and $(2, 2, 0)$ charge reflections at the Gd L_{II} and L_{III} edges. Fig. 4 shows, at selected T , energy scans over the Gd L_{II} and L_{III} edges for the satellite reflections at $(4 - \tau, 4 - \tau, 0)$. The position and the peak shape of the resonances for both L_{II} and L_{III} edges is T independent within our resolution and consistent with dipolar (E_1) transitions.^{7,22,23,24} When τ is small, the magnetic peak position is closer to the charge peak increasing the background. Since τ is T dependent the background varies with T as well. Furthermore, at the Gd L_{III} edge, the angle of the analyzer crystal for the polarization analysis is further away from the ideal 90° for rejection of the charge scattering component than in the case of the L_{II} edge, resulting in a higher charge-scattering background at the L_{III} edge.

The specific heat discussed above implies that in the HTP the Gd 4f moments are not ordered. Since XRMS is element-sensitive, this might seem in contradiction to our observation of a resonant magnetic signal at the Gd L edges at 55 and 130 K (Fig. 4 ■ and ○). However, XRMS (E_1) on the Gd L edges is sensitive to the polarization of the Gd 5d bands, not (directly) to its 4f moments.^{7,22,23,24} A Gd 5d band polarization can also be induced by the Fe 3d moments. For this situation, a very weak intensity for the corresponding magnetic satellites has to be expected.²⁵ Compared to other Gd compounds,^{26,27} the intensity I of the satellite reflections we observed is indeed very weak – more than three orders

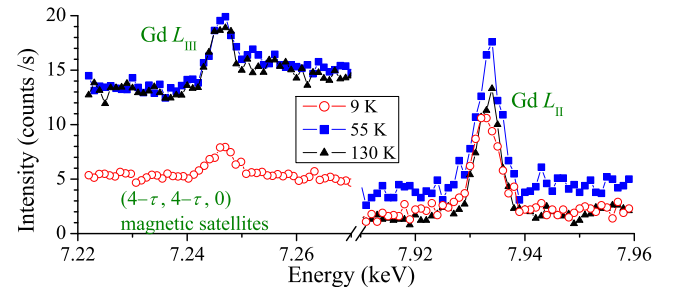


FIG. 4: (Color online) Energy scans of the intensity of the $(4 - \tau, 4 - \tau, 0)$ satellite reflections, at 9 K (○, $\tau = 0.133$), 55 K (■, $\tau = 0.067$), and 130 K (▲, $\tau = 0.086$).

of magnitude lower. Changing the azimuthal angle^{7,27} did not significantly change I , suggesting that its low value is not related to the direction of magnetic moments. The reason for the Gd 4f moments not to follow the order of its 5d band polarization may be that the 5d polarization is too weak at high T to force the 4f moments into a long range ordered state – similar to the situation in Dy148 at high T .⁷ Based on this discussion, although we did not observe a clear resonant enhancement at the Fe K edge, we conclude that the $(\tau, \tau, 0)$ propagation vector describes the order of the Fe moments. That this Fe moment modulation is along [110] is common for R148 compounds, but in other R148 τ is typically larger ($0.127 < \tau < 0.243$) and varies less with T .^{8,9,10,11}

At 9 K, the satellite reflections are present as well (Fig. 4). This fact, and the smooth variation with T of the position of the $(\tau, \tau, 0)$ propagation vector, demonstrate that the Fe moments keep their modulation from the HTP, where the Gd 4f moments are not ordered, in the LTP, where the Gd 4f moments *are* ordered. This is similar to the situation in other R148 compounds. However, the low intensity of the $(4 - \tau, 4 - \tau, 0)$ satellite reflections at low T indicate that for Gd148, unlike the situation in other R148 compounds,^{7,8,10} the rare-earth 4f moments do *not* follow the Fe moment modulation. Additionally, we found (at 9 K, L_{II}) a magnetic satellite reflection at $(2, 2, 0.3)$, corresponding to a propagation vector of $(0, 0, 0.3)$. While limited beam time did not permit us to track this propagation vector in T or measure any other satellite reflections associated with this propagation vector, it may be associated with a Gd 4f antiferromagnetic modulation, and is probably related to the (low H) linear $M(H)$ behavior for $H \parallel [001]$ in the LTP.

Regardless of the exact distribution of the Gd 4f moment in ferromagnetic and antiferromagnetic orders, the fact that these moments do not follow the Fe modulation implies that they order independently, leading to a *co-existence of two distinct orders*. Our thermodynamic and transport measurements are consistent with this picture, e.g. the existence of spontaneous ferromagnetic moments is also incompatible with Gd 4f moments simply following the antiferromagnetic Fe 3d order. However, there

are several questions remaining, including the question of how to account for the full Gd 4f moment of $7\mu_B$. To resolve these questions, additional scattering and thermodynamic experiments are planned. Particularly, we will better characterize the (0,0,0.3) modulation, and search intensively for a Fe K edge resonant signal, which is difficult to observe due to the nature of the associated transition into a p-state.

The ferromagnetic order of Gd 4f moments below T_2 , and additional antiferromagnetic order with modulation in [001] direction coexisting with the *distinct* antiferromagnetic order of the Fe 3d moments is the central point of our paper. It may indicate a modified relation between the strength of the Gd 4f-Gd 4f and Gd 4f-Fe 3d interactions in Gd148 as compared to other R148 compounds. As we mentioned, apart from the stronger couplings between 4f and conduction electrons in general, the most peculiar property of Gd is the absence of crystal-electric-field effects.

It seems remarkable that in the absence of the MCA due to crystal electric field effects, the magnetic behavior in Gd148 is *more* complex than in other R148. Likely, strong crystal-electric-field effects play a central role in the magnetism in R148 (except for Gd148). E.g., in Dy148, crystal-electric-field effects press the 4f moments

into the plane, making an order following the Fe-moment modulation more probable. Our results on Gd148, in contrast, indicate a complex interplay of 4f and 3d moments when crystal-electric-field effects are absent.

In conclusion, two transitions at $T_1 = 21\text{ K}$ and $T_2 = 27\text{ K}$ at low temperature divide the ordered state below $T_N = 155\text{ K}$, where Fe moments order antiferromagnetically, into three phases. Gd 4f moments order below T_2 , with a ferromagnetic component. The Gd 4f moment order is distinct from the Fe-moment order. Below T_1 the moments have an in-plane ferromagnetic component but seem antiferromagnetic out-of-plane. The complex magnetism in GdFe₄Al₈ likely is related to a modified ratio of coupling strengths and the absence of crystal-electric-field effects.

We thank S. L. Bud'ko and R. W. McCallum for useful discussions. Ames Laboratory is operated for the U.S. Department of Energy by Iowa State University under Contract No. W-7405-Eng-82. This work was supported by the Director for Energy Research, Office of Basic Energy Sciences. Synchrotron work was performed at the MuCAT sector at the Advanced Photon Source supported by the U.S. DOE, BES, and OS under Contract No. W-31-109-Eng-38.

* Email: angst@ameslab.gov

† Current address: Institut für Festkörperphysik, Technische Universität Dresden, 01062 Dresden, Germany

¹ I. A. Campbell, J. Phys. F: Metal Phys. **2**, L47 (1972).

² K. H. J. Buschow and A. M. van der Kraan, J. Phys. F: Met. Phys. **8**, 921 (1978).

³ I. Felner and I. Nowik, J. Phys. Chem. Solids **39**, 951 (1978).

⁴ H. Fujiwara, W.-L. Liu, H. Kadomatsu, and T. Tokunaga, J. Magn. Magn. Mater. **70**, 301 (1987).

⁵ N. P. Duong, E. Brück, F. R. de Boer, and K. H. J. Buschow, Physica B **294-295**, 212 (2001).

⁶ N. P. Duong, E. Brück, P. E. Brommer, A. de Visser, F. R. de Boer, and K. H. J. Buschow, Phys. Rev. B **65**, 020408(R) (2001).

⁷ S. Langridge, J. A. Paixão, N. Bernhoeft, C. Vettier, G. H. Lander, D. Gibbs, S. A. Sørensen, A. Stunault, D. Wermeille, and E. Talik, Phys. Rev. Lett. **82**, 2187 (1999).

⁸ J. A. Paixão, M. Ramos Silva, S. A. Sørensen, B. Lebech, G. H. Lander, P. J. Brown, S. Langridge, E. Talik, and A. P. Gonçalves, Phys. Rev. B **61**, 6176 (2000).

⁹ J. A. Paixão, M. R. Silva, J. C. Waerenborgh, A. P. Gonçalves, G. H. Lander, P. J. Brown, M. Godinho, and P. Burlet, Phys. Rev. B **63**, 054410 (2001).

¹⁰ P. Schobinger-Papamantellos, K. H. J. Buschow, and C. Ritter, J. Magn. Magn. Mater. **186**, 21 (1998).

¹¹ P. Schobinger-Papamantellos, K. H. J. Buschow, I. H. Hagemusa, F. R. de Boer, C. Ritter, and F. Fauth, J. Magn. Magn. Mater. **202**, 410 (1999).

¹² Z. Fisk and J. P. Remieka, in *Handbook on the Physics and Chemistry of Rare Earths* (Elsevier, Amsterdam, 1989), Vol. 12.

¹³ P. C. Canfield and Z. Fisk, Phil. Mag. B **65**, 1117 (1992).

¹⁴ P. C. Canfield and I. R. Fisher, J. Crystal Growth **225**, 155 (2001).

¹⁵ M. Angst *et al.*, unpublished.

¹⁶ Consistent with measurements on polycrystalline Gd148. See Palasyuk *et al.*, J. Alloys Compd. **367**, 205 (2004).

¹⁷ Indications for a transition around 20 K (but not its first order nature) were earlier found by Fujiwara *et al.*⁴ Their torque measurements indicate a change of the angle between the magnetic easy axis and the *ab* plane from $\sim 30^\circ$ at high T to 0° at low T .

¹⁸ I. H. Hagemusa, E. Brück, F. R. de Boer, and K. H. J. Buschow, J. Alloys Compd. **278**, 80 (1998).

¹⁹ A. R. Mackintosh, Phys. Rev. Lett. **9**, 90 (1962).

²⁰ A. Mauger, M. Escorne, and D. Ravot, Phys. Rev. B **39**, 6934 (1989).

²¹ K. J. Singh, S. Chaudhary, M. K. Chattopadhyay, M. A. Manekar, S. B. Roy, and P. Chaddah, Phys. Rev. B **65**, 094419 (2002).

²² D. Gibbs, D. R. Harshman, E. D. Isaacs, D. B. McWhan, D. Mills, and C. Vettier, Phys. Rev. Lett. **61**, 1241 (1988).

²³ J. P. Hannon, G. T. Trammell, M. Blume, and D. Gibbs, Phys. Rev. Lett. **61**, 1245 (1988).

²⁴ For a recent review see articles in Synchrotron Radiation News, Vol. 14, No. 5 (2001).

²⁵ B. A. Everitt, M. B. Salamon, B. J. Park, C. P. Flynn, T. Thurston, and D. Gibbs, Phys. Rev. Lett. **75**, 3182 (1995).

²⁶ E. Granado, P. G. Pagliuso, C. Giles, R. Lora-Serrano, F. Yokaichiya, and J. L. Sarrao, Phys. Rev. B **69**, 144411 (2004).

²⁷ L. Tan, A. Kreyssig, J. W. Kim, A. I. Goldman, R. J. McQueeney, D. Wermeille, B. Sieve, T. A. Lograsso, D. L.

Schlagel, S. L. Bud'ko, V. K. Pecharsky, and K. A. Gschneider, Jr., Phys. Rev. B (to be published).